SUPPORTING INFORMATION

Battling Btk Mutants With Noncovalent Inhibitors That Overcome Cys481 and Thr474 Mutations

Adam R. Johnson,*[,†] Pawan Bir Kohli,[†] Arna Katewa,[‡] Emily Gogol,[‡] Lisa D. Belmont,[§] Regina Choy,[§] Elicia Penuel,[#] Luciana Burton,[#] Charles Eigenbrot,[¶] Christine Yu,[¶] Daniel F. Ortwine,[‖] Krista Bowman,[¶] Yvonne Franke,[¶] Christine Tam,[¶] Alberto Estevez,[¶] Kyle Mortara,[¶] Jiansheng Wu,[¶] Hong Li,[¶] May Lin,[¶] Philippe Bergeron,[%] James J. Crawford,[%] and Wendy B. Young [%]

[†]Biochemical and Cellular Pharmacology, Genentech, 1 DNA Way, South San Francisco, California 94080

[‡]Discovery Immunology, Genentech, 1 DNA Way, South San Francisco, California 94080

[§]Discovery Oncology, Genentech, 1 DNA Way, South San Francisco, California 94080

[#]Biomarker Development, Genentech, 1 DNA Way, South San Francisco, California 94080

[¶]Protein Chemistry and Structural Biology, Genentech, 1 DNA Way, South San Francisco, California 94080

[‖]Computational Chemistry, Genentech, 1 DNA Way, South San Francisco, California 94080

[%]Discovery Chemistry, Genentech, 1 DNA Way, South San Francisco, California 94080

* Correspondence: johnsa26@gene.com

METHODS

Btk proteins. Purified recombinant human full-length catalytically active WT Btk protein that had been expressed in baculovirus-infected insect cells was obtained from Carna Biosciences and used as supplied. Mutant Btk proteins (C481S, C481R, T474I and T474M) were generated at Genentech by standard molecular biology techniques, expressed in baculovirus-infected insect cells, and purified. The Btk gene (Ala2–Ser659) was subcloned into a modified pAcGP67A vector (BD Biosciences) behind the polyhedron promoter with an N-terminal His-tag and a C-terminal His-tag, respectively, for expression in insect cells. Individual point mutations were introduced by site-directed mutagenesis using standard QuikChange protocols (Agilent Technologies). The integrity of all expression constructs was confirmed by DNA sequencing. Transfer vectors were co-transfected with BestBac linearized viral DNA (Expression Systems, LLC) into *Spodoptera frugiperda* 9 (*Sf*9) cells using Cellfectin (Invitrogen) to produce recombinant baculovirus. The virus was amplified twice to prepare the stock used for protein expression. Btk mutant C481S was expressed in *Sf*9 cells and all other mutant Btk proteins were expressed in *Trichoplusia ni* pro cells. Shake flasks (5 L; Thompson Instrument Company) were inoculated with 2 L of *Sf*9 or *T. ni* pro cells (Expression Systems, LLC) at 1E6 cells/mL in serum-free ESF921 medium (Expression Systems, LLC). The cells were grown at 27 °C and 120 rpm to a density of 2E6 cells/mL and infected with the appropriate virus at a ratio of virus/culture of 2.5 mL/L (v/v) for *Sf*9 cells and 5 mL/L (v/v) for *T. ni* pro cells. After 2 or 3 days post-infection for *Sf9* or *T. ni pro* cell cultures, respectively, cells expressing protein were harvested by centrifugation at 4000*g* for 15 min and frozen at –80 °C until purification. A common protocol was used to purify the His-tagged Btk proteins. Cells were lysed in 50 mM Tris-HCl buffer (pH 8.5), containing 150 mM NaCl, 20 mM imidazole, 1 mM TCEP, and Complete EDTA-free protease inhibitor (Roche) by stirring at 4 °C for 1 hr. The lysate was subjected to ultracentrifugation at 40000*g* for 1 hr. The supernatant fluid was filtered and then loaded onto a 3-mL Ni^{2+}-charged NTA column (Qiagen NiNTA superflow) that had been equilibrated in Buffer A [20 mM Tris-HCl buffer (pH 8.5), 300 mM NaCl, 20 mM imidazole, and 0.5 mM TCEP]. The bound protein was eluted in Buffer A containing 250 mM imidazole (instead of 20 mM). The eluted protein was concentrated and then further

purified by size exclusion chromatography on a 120-mL Superdex 200 16/60 column (GE Healthcare) that had been equilibrated with 20 mM Tris-HCl buffer (pH 8.5), containing 200 mM NaCl, 10% glycerol, and 0.5 mM TCEP. The eluted protein fractions were analyzed by SDS-PAGE and pooled to provide protein preparations that were frozen.

Inhibitors. Inhibitors **1a** and **2** were obtained commercially. Compounds **3a** and **3c** were synthesized as described (*1*) and **4** was prepared as published (*2*). Inhibitors **5**–**9** were synthesized as reported previously (*3*,*4*), while **1b** and **3b** were prepared as shown below.

Synthesis of **1b**:

1-[(3*R*)-3-[4-amino-3-(4-phenoxyphenyl)-pyrazolo[3,4-d]pyrimidin-1-yl]-1-piperidyl]propan-1-one

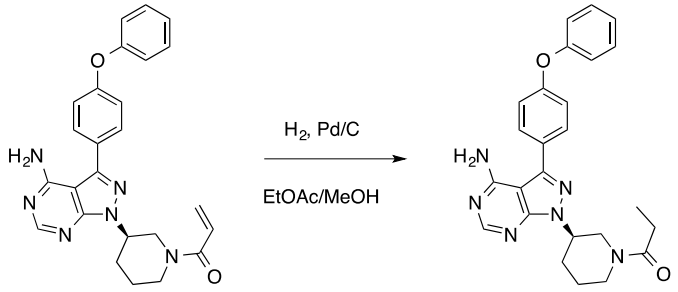

1a **1b**

A mixture of 1-[(3*R*)-3-[4-amino-3-(4-phenoxyphenyl) pyrazolo[3,4-d]pyrimidin-1-yl]-1-piperidyl]prop-2-en-1-one (**1a**) (75 mg, 0.17 mmol) and palladium, 10% on Carbon (0.017 mmol, 18 mg) was suspended in a mixture of ethyl acetate (1 mL) and methanol (2 mL). The mixture was vacuum purged for 2 min and the atmosphere was replaced with H_2. The mixture was stirred under hydrogen at room temperature overnight then filtered through Celite, and the filtrand washed with DCM. The filtrate was concentrated under reduced pressure and the residue was purified by reverse-phase prep-HPLC to afford the title compound as a white solid (70.2 mg, 93%). MS-ESI: $[M+H]^+$ 443.2

^{1}H NMR (400 MHz, DMSO-d6) δ 8.26 (d, *J* = 9.1 Hz, 1H), 7.66 (d, *J* = 8.3 Hz, 2H), 7.48–7.39 (m, 2H), 7.23–7.09 (m, 5H), 4.86–4.40 (m, 2H), 4.32–3.45 (m, 2H), 3.11 (q, *J*

= 11.0 Hz, 1H), 2.37 (s, 2H), 2.27–2.20 (m, 2H), 2.20–2.05 (m, 1H), 1.95–1.75 (m, 1H), 1.73–1.41 (m, 1H), 1.02–0.95 (m, 3H).

Synthesis of **3b**:

(*R*)-6-amino-7-(4-phenoxyphenyl)-9-(1-propionylpyrrolidin-3-yl)-7H-purin-8(9H)-one

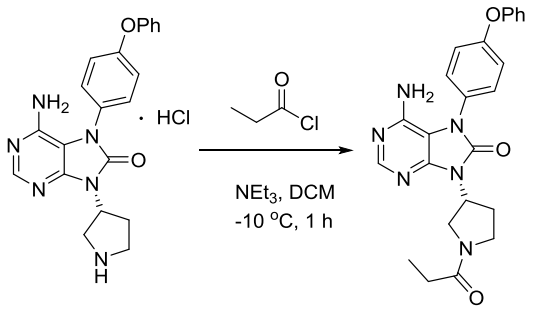

3b

To a solution of (*R*)-6-amino-7-(4-phenoxyphenyl)-9-(pyrrolidin-3-yl)-7H-purin-8(9H)-one hydrochloride (*1*) (47.8 mg, 0.123 mmol) in DCM (2 mL) cooled at –10 °C was added Et_3N (37.2 mg, 0.369 mmol). After stirring for 10 min, a solution of propionyl chloride (13.6 mg, 0.147 mmol) in DCM (1 mL) was added and the reaction mixture was stirred at –10 °C for 1 h. It was then concentrated under reduced pressure and the residue was purified by reverse-phase prep-HPLC to afford the title compound as a white solid (22.4 mg, 41%, 2 steps). MS-ESI: $[M+H]^+$ 445.3

^{1}H NMR (500 MHz, $CDCl_3$) δ 8.26 (d, *J* = 12.0 Hz, 1H), 7.45–7.40 (m, 4H), 7.23–7.22 (m, 1H), 7.16–7.11 (m, 4H), 5.30–5.20 (m, 1H), 4.53–4.51 (m, 2H), 4.22–4.08 (m, 1H), 4.00–3.79 (m, 2H), 3.58–3.50 (m, 1H), 3.01–2.81 (m, 1H), 2.38–2.31 (m, 3H), 1.21–1.11 (m, 3H).

Btk kinase activity assay and inhibitor testing. We measured Btk-catalyzed tyrosine phosphorylation of a synthetic peptide (5-FAM-EEPLYWSFPAKKK-NH_2; ProfilerPro® FL-Peptide 22; Product 760366; PerkinElmer) using a LabChip 3000® microfluidic mobility shift instrument (PerkinElmer) in the in vitro biochemical assay. For determination of the apparent K_m for ATP, reaction mixtures contained 50 mM

HEPES buffer (pH 7.5), 10 mM $MgCl_2$, 0.01% Triton X-100, 1 mM dithiothreitol, 1 μM FL-Peptide 22, 0–500 μM ATP, and 1 or 2 nM total Btk protein. For the low activity C481R, the total kinase concentration was increased to 30 nM to achieve 10–20% conversion of peptide substrate to phospho-peptide product. For the inhibition studies, reaction mixtures contained the same components as above, but the ATP concentration was fixed at 45 μM near the K_m for WT, and the reactions contained a titration of up to 10,000 nM test article in a final concentration of 0.5% (v/v) DMSO. In each titration, the test article was tested in duplicate at 12 concentrations. Blank reactions contained ATP, peptide, and DMSO, but no Btk or test article, whereas uninhibited control reactions contained ATP, peptide, Btk, and DMSO, but no test article. For both the K_m experiments and the inhibition experiments, kinase reactions were incubated for 30 min at room temperature (22–23 °C) in a final volume of 20 μL per well in 384-well plates.
Ten microliters of Btk plus peptide mixture were added to 10 μL of a mixture of ATP and test article (or vehicle) to initiate the reactions. Duplicate inhibitor titrations were used to generate each IC_{50}. Reactions were stopped by adding 10 μL of 0.25 M EDTA (pH 8.0) to each well. In each reaction, the residual FL-Peptide 22 substrate (S) and the phospho-peptide product (P) generated were separated and quantified using the LabChip 3000. Electrophoretic separation of molecules of product from molecules of substrate was achieved using downstream and upstream voltages of –500 and –2250 V, respectively, at an operating pressure of –1 psi. The 5-FAM group present on both the substrate and product peptides was excited at 488 nm; the fluorescence at 530 nm was detected and the peak heights were reported. The extent (or percent) of conversion of substrate to product was calculated from the corresponding peak heights in the electropherogram using HTS Well Analyzer software, version 5.2 (PerkinElmer) and the following equation

$$\%\ \text{conversion} = \frac{P}{S + P} \times 100$$

where P and S represent the peak heights of the product and substrate, respectively. After any baseline signal from blank wells containing no Btk was subtracted from the signal of all test wells, the % conversion data were converted to % of Control. The % conversion

observed in uninhibited control reaction wells containing Btk and DMSO vehicle was defined as 100% of Control while blank wells with no Btk were defined as 0% of Control. The % of Control data were plotted against the log of the inhibitor concentration and fit by non-linear regression using Prism v5.0 (GraphPad software) to the variable slope 4-parameter sigmoidal inhibition equation to determine IC_{50}.

Protein expression and purification for crystallography. Codon optimized DNA encoding residues Gly393–Glu657 of Btk followed by a TEV cleavage site and a His_6-tag at the C-terminus was cloned into a pBacgus-1 transfer vector (Novagen). Amplified virus was used to express protein in *Sf*9 cells over 72 hr. Cells were suspended in 50 mM CHES buffer (pH 9.0) containing 250 mM NaCl, 0.25% NP-40, 1 mM TCEP, 10 mM imidazole, and a cocktail of protease inhibitors and then lysed using a microfluidizer. The resultant lysate was clarified by centrifugation at 40,000 rpm for 1 hr. The supernatant fluid was incubated with Ni-NTA superflow beads (QIAGEN) and the slurry was poured into a gravity fed Econo column. The column was washed with 10 column volumes of 20 mM CHES buffer (pH 9.0) containing 200 mM NaCl, 1 mM TCEP, and 20 mM imidazole and then eluted with buffer containing 300 mM imidazole. The eluent was incubated overnight at 4 °C with TEV protease to cleave the C-terminal His_6 tags while being buffer-exchanged via dialysis into 20 mM Tris-HCl buffer (pH 8.5) containing 200 mM NaCl, and 1 mM TCEP. The cleaved, dialyzed sample was loaded onto a second Ni-NTA column to remove non-cleaved protein, and the flow through was further purified by gel filtration on a Superdex 75 column (GE Healthcare) that had been equilibrated in 20 mM Tris-HCl buffer (pH 8.5) containing 100 mM NaCl, and 0.5 mM TCEP. Purified Btk was then concentrated to ~10 mg/mL.

Crystallization, data collection and refinement of Btk/Compound 9. The purified Btk at ~10 mg/mL was incubated at 4 °C for 2 hr with a 2-fold molar excess of **9**. Crystals were grown at 13 °C by vapor diffusion in hanging drops containing equal volumes of protein and reservoir solution [6% PEG 10,000 in 100 mM citrate buffer (pH 5.5) containing 100 mM Li_2SO_4]. Larger crystals were obtained by streak seeding. Crystals were cryoprotected in reservoir solution supplemented with 25% glycerol. Diffraction data were collected at APS beamline 21-IDF (LS-CAT) and reduced using HKL2000 (*5*)

and elements of the CCP4 suite (*6*) in a hexagonal space group. Initial phases were available from a high-resolution isomorphous Btk structure (3OCS) in the PDB (*7*). Model building was performed using Coot (*8*) and refinement employed both Refmac5 (*9*) and phenix.refine (*10*). Metrics characterizing the data and final model appear in Table S1. The X-ray co-crystal structural data set has been deposited in the PDB as accession ID code 5KUP.

Protein-inhibitor structure modeling. A model of **1a** covalently bound to the Btk active site was built using the X-ray crystal structure of Btk bound to a related inhibitor analog (PDB 4YHF) (*11*). A model of **6** in the Btk binding site was built using the co-crystal structure of Btk with **9** from the present work (PDB: 5KUP). Models were constructed using the MOE software v2016.10 (www.chemcorp.com) and ligands were minimized in the active site using default parameter settings. The H3 selectivity pocket was depicted using the Molecular Surface function within MOE v2015.10 to contour the surfaces of Btk residues within 3.5 Å of any atom of the fluorophenyl ring of **9** and its *t*-butyl substituent. Specifically, residues Gln412, Phe413, Gln421, His519, Asp521, Asn526, Leu542, Ser543, and Tyr551 were used to create the surface.

Human whole blood assay of CD69 expression. Heparinized whole blood (100 μL) from healthy human volunteers was dispensed into 96-well square top/tapered V-bottom deep-well plates and incubated for 1 h at 37 °C with an 11-point titration (3-fold serial dilutions) of inhibitor starting at a top concentration of 4.76 μM or DMSO vehicle in duplicate. Blood was then stimulated 18 h in the presence of 50 μg/mL of goat anti-IgM $F(ab')_2$ (SouthernBiotech). After the incubation, B cells were stained with anti-mouse CD19 PerCP (BD Biosciences, clone SJ25C1), anti-mouse CD27 FITC (BD Biosciences, clone L128) and anti-mouse CD69 PE (BD Biosciences, clone FN50) or Isotype IgG1 PE antibodies for 30 min at room temperature followed by RBC lysis using 1X BD lysis buffer. Cells were washed with FACS buffer and fixed with 2% paraformaldehyde. Samples were acquired on BD LSRII and analyzed using BD FACSDiva software. B cells were gated as $CD19^{+}CD27^{-}$ and B-cell activation was assessed based on CD69 PE mean fluorescence intensity (MFI). CD69 MFI was plotted vs. the logarithm of the

inhibitor concentration and the MFI data were fit by non-linear regression using Prism v5.0 to the variable slope 4-parameter sigmoidal inhibition equation to determine the IC_{50}. Each compound was tested in duplicate with blood from at least 3 different donors.

Cellular assay of Btk phosphorylation. Rabbit anti-α-tubulin (mAb) (2125; Cell Signaling Technology, Inc.), rabbit anti-pY223-Btk mAb (Epitomics), rabbit anti-Btk (26560002, Novus Biologicals) were commercially available. HEK293T cells were transfected with plasmid encoding either WT or C481S mutant Btk with a C-terminal 6-His tag. Transfected cells were treated with vehicle (DMSO) or 1 μM inhibitor in vehicle for 5 h and stimulated for 5 min at room temperature with 10 μg/mL goat $F(ab')_2$ anti-human IgM-LE/AF (2022-14, SouthernBiotech) followed by a wash with cold PBS to terminate the stimulation. The cell pellet was lysed in cold RIPA buffer (R0278, Sigma-Aldrich) containing protease inhibitors (11697498001, Sigma-Aldrich) and phosphatase inhibitors 1 and 2 (P5726 and P0044, Sigma-Aldrich). Protein extracts were lysed 30 min at 4 °C, then centrifuged at 10,000*g* for 10 min at 4 °C. Protein concentrations were measured by the Pierce BCA Protein Assay Kit (23227, Thermo Scientific) using bovine serum albumin for the standard curve. For WES™ automated western blotting, all reagents and samples were prepared and used according to manufacturer's user guide [Wes-Rabbit Master Kit (12–230 kD) (PS-MK01, Protein Simple)]. Briefly, 0.5 μg of total cellular protein lysate was mixed with 5x fluorescent master mix containing SDS, DTT, and three biotin-labeled protein standards with molecular weights of 1, 29 and 180 kD, and incubated for 5 min at 95 °C. The treated samples, biotin-labeled molecular weight ladder, blocking reagent, wash buffer, primary antibodies, secondary antibodies, and chemiluminescent substrate were dispensed into designated wells in the 25-well sample plate provided. The plate was loaded into the WES instrument and automated separation capillary electrophoresis and immunodetection was performed using default settings. Data analysis was performed using the WES Compass v2.5.11 Software. Statistical analysis of significance between groups was done by unpaired t-test of significance at 95% confidence interval with Prism v5.0 (GraphPad Software).

Table S1. Data collection and refinement statistics for the human Btk(393–657)/Compound **9** co-crystal structure

	Compound **9**
Data collection & reduction	
X-ray source	APS 21-ID-F
Wavelength (Å)	0.9787
Resolution range (Å)	35.47–1.39 (1.44–1.39)
Space group	$P6_1$
Unit cell edges (Å)	108.373 108.373 42.453
Unit cell angles (˚)	90 90 120
Total reflections	465465
Unique reflections	56763 (5544)
Multiplicity	8.2 (7.7)
Completeness (%)	98.47 (97.02)
Mean I/sigma(I)	28.0 (2.6)
Wilson B-factor ($Å^2$)	14.42
R-symm	0.075 (0.897)
Refinement	
Reflections used for R-free	2919
R-work	0.165 (0.237)
R-free	0.177 (0.242)
Number of non-H atoms	2654
macromolecules	2266
ligands	69
water	319
Protein residues	265
RMS(bonds) (Å)	0.006
RMS(angles) (˚)	1.17
Ramachandran favored (%)	97
Average B-factor ($Å^2$)	19.8
macromolecules	18.0
ligands	22.2
solvent	31.9

Figure S1. Steady state kinetics Michaelis-Menten plots of the Btk enzyme forms used in this work. Data from a single titration for each enzyme are shown. Note that the ordinate scale for C481R is one-tenth that of the other plots.

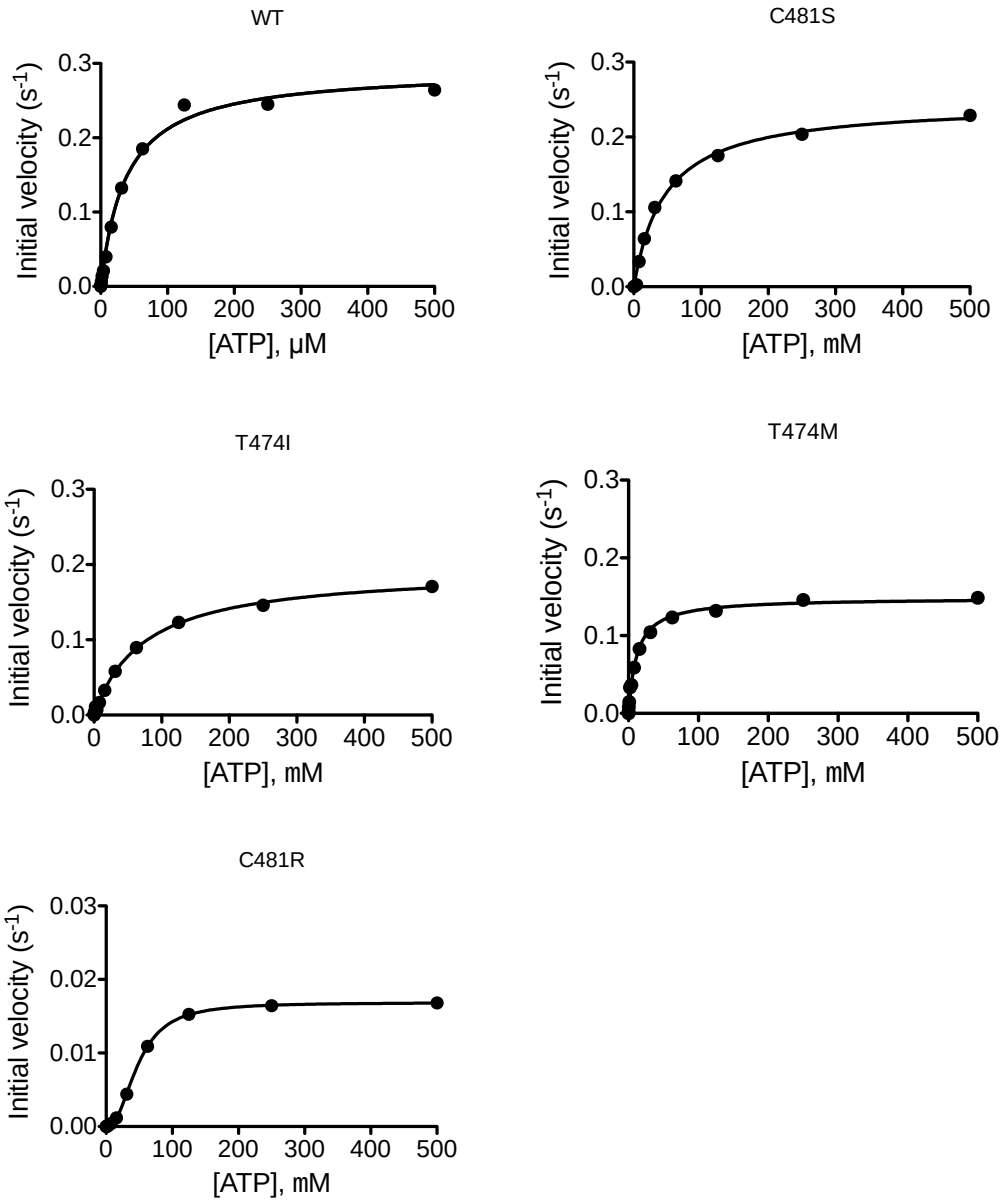

Figure S2. Kinase selectivity of the Btk inhibitors. ATP concentrations used were either at the apparent K_m (K_m app) or as listed (μM) in the column [ATP]; NA (not applicable) denotes competitive binding assays that contained no ATP. The % Inhibition by 1 μM inhibitor is shown. The color scheme is the same as used in Figure 4a. NT, Not Tested.

		% Inhibition by Inhibitor										
Kinase	**[ATP]**	**1a**	**1b**	**2**	**3a**	**3c**	**4**	**5**	**6**	**7**	**8**	**9**
Abl	Km app	39	21	23	6	-5	12	30	23	2	13	19
ACVR1B	Km app	0	1	2	2	-4	-5	0	6	1	5	-5
ACVR2B	NA	2	5	14	8	0	7	6	6	1	7	5
AKT1	Km app	8	6	1	2	1	2	3	5	1	4	1
AKT2	Km app	3	3	8	0	-1	1	4	4	4	3	11
ALK2	NA	14	5	41	1	-1	1	2	-1	1	3	3
ARK5	Km app	2	19	72	-5	-3	-15	-10	3	11	6	-1
ASK1	NA	5	2	6	4	-6	2	2	1	5	8	3
Aurora_A	Km app	45	24	59	-1	-4	5	9	21	-2	12	7
Aurora_B	Km app	18	15	57	1	-1	5	3	5	3	-2	-1
Axl	Km app	9	5	13	-5	-9	3	0	4	6	-4	1
B-Raf	NA	59	51	6	27	24	28	0	4	1	0	3
Blk	Km app	102	96	44	99	47	16	17	13	-2	6	14
BMPR1A	NA	-1	-3	4	-2	0	11	-2	5	-1	17	3
Bmx	Km app	99	98	99	98	97	77	58	88	49	34	15
Brk	Km app	100	95	14	60	39	39	6	77	-2	3	2
BrSK1	Km app	1	-1	10	0	0	8	-1	4	-2	1	2
BTK	Km app	101	100	100	99	98	100	96	99	102	94	94
CaMKI	100	-7	16	-10	13	7	-2	-15	4	-10	17	18
CaMKI_delta	Km app	8	11	7	1	0	4	7	3	6	7	-2
CamKII_alpha	Km app	-2	-2	-4	5	2	-2	-1	1	9	-7	1
CaMKII_beta	Km app	13	12	4	10	6	-3	9	-5	2	10	9
CamKIV	Km app	8	10	-2	2	-5	4	11	6	-3	15	8
CAMKK1	NA	-12	-8	2	-2	6	-7	-9	-6	1	-7	-7
CAMKK2	NA	-1	-3	8	2	2	2	4	4	3	0	6
CDK1/cyclinB	Km app	6	1	6	5	7	6	6	2	6	7	5
CDK2/cyclinA	Km app	2	-1	0	-3	-3	7	2	6	0	3	4
CDK5/p25	Km app	2	2	1	3	-6	16	-9	-7	5	6	-1
CDK7/cyclinH	Km app	-20	-2	0	-2	-2	7	-5	-6	15	-8	4
CDK8/cyclinC	NA	14	12	15	14	10	19	-5	2	17	-4	7
CDK9/cyclinT1	Km app	1	-7	-3	-2	-1	36	-12	8	-9	10	-2
CHK1	Km app	2	2	0	-7	-7	-4	6	6	-1	-2	4
CHK2	Km app	12	9	6	-4	-2	3	2	5	3	8	-1
CK1_alpha1	Km app	2	-1	1	2	-1	1	1	2	-13	5	-2
CK1_delta	Km app	8	7	-2	4	1	7	6	5	-2	10	5
CK1_epsilon1	Km app	32	37	-3	17	10	3	5	2	1	3	1
CK1_gamma1	Km app	-3	1	-4	1	1	-4	-20	-5	-1	-14	11
CK1_gamma2	Km app	2	-1	1	7	1	1	11	-1	-1	8	7
CK2_alpha1	Km app	2	8	7	15	4	-2	-1	6	7	6	5
CLK1	Km app	-4	3	3	3	2	3	-1	4	1	-2	1
CLK2	Km app	-2	-2	35	-7	-6	3	-6	6	6	1	-2
CLK3	Km app	5	5	0	3	1	2	6	1	0	6	3
CLK4	NA	6	5	49	6	8	7	5	2	1	5	3
Cot	100	30	18	25	16	5	9	18	8	8	11	8
CSF1R	Km app	55	58	24	3	2	-4	3	16	-5	-2	-1
CSK	Km app	98	97	11	63	48	8	9	11	5	8	7
DAPK1	Km app	27	22	0	7	4	7	21	-7	6	18	-20
DCAMKL2	Km app	7	5	-1	-2	1	2	-5	7	-1	2	3
DDR1	NA	2	2	5	4	-1	3	-3	-1	5	5	6
DMPK	NA	-8	-14	1	-1	-6	-1	-3	8	-3	-10	1
DNA-PK	Km app	11	10	2	9	7	-1	3	11	3	7	3
DRAK1	NA	4	1	56	1	7	6	5	2	5	5	6
DYRK1A	Km app	4	5	-3	-1	-2	9	7	2	-2	10	10
DYRK3	Km app	4	-2	5	-3	-4	0	4	4	4	0	1
DYRK4	Km app	-1	0	-1	4	0	2	-2	3	-1	0	-1
eEF-2K	Km app	-3	3	9	5	8	7	-3	4	5	3	9
EGFR	Km app	89	20	34	72	-2	-1	-3	4	3	-8	-2
EGFR(T790M,L858R)	Km app	26	4	52	-1	-2	6	0	6	8	6	0
EphA1	Km app	30	31	19	11	5	9	4	6	1	6	2
EphA3	NA	12	13	5	10	2	2	6	-3	2	9	5
EphA7	NA	18	14	21	4	0	3	5	6	4	9	13
EphA8	Km app	48	41	0	7	2	5	1	2	-4	-8	3
EphB1	Km app	7	9	8	2	0	2	-1	6	1	5	1
EphB3	Km app	3	2	-1	3	-1	3	1	0	-2	1	3
ErbB2	Km app	91	50	6	56	7	36	6	3	-7	7	-1
ErbB4	Km app	93	86	76	101	28	93	2	25	0	3	3
ERK2	Km app	11	8	8	6	5	3	7	4	8	4	2
FAK	Km app	-3	4	14	-7	-4	-3	3	4	4	3	11
Fes	Km app	5	-5	25	8	4	2	1	2	2	-3	10
FGFR1	Km app	53	52	16	5	1	0	9	1	11	3	5
FGFR3	Km app	31	29	16	10	6	-4	10	0	27	4	-1
FGFR4	Km app	22	19	4	9	1	-1	11	4	18	-1	6

		% Inhibition by Inhibitor										
Kinase	**[ATP]**	**1a**	**1b**	**2**	**3a**	**3c**	**4**	**5**	**6**	**7**	**8**	**9**
Fgr	Km app	103	102	40	81	73	30	78	76	66	45	38
Flt1	Km app	22	19	8	3	2	4	1	2	3	6	1
Flt3	Km app	86	85	61	14	12	7	13	16	1	7	9
Flt4	Km app	69	73	51	7	3	8	16	12	6	15	10
Frk	Km app	88	82	8	20	10	36	15	10	5	3	11
GRK2	Km app	-5	-1	0	-1	0	-3	-4	-3	1	-1	11
GRK3	Km app	-5	4	-2	-2	-3	-2	3	-2	-3	0	10
GRK5	Km app	-1	2	-5	-4	-4	-7	-3	-2	-1	-1	-1
GRK6	Km app	1	5	-1	4	-1	0	8	-1	-2	9	3
GSK3_alpha	Km app	15	8	1	4	-1	2	4	4	2	7	6
GSK3_beta	Km app	-1	0	6	-6	-7	2	-2	4	4	2	9
Hck	Km app	98	94	31	NT	31	3	48	8	15	14	10
HIPK1	Km app	0	3	-1	1	-1	-3	4	-1	-3	0	0
HIPK2	Km app	3	3	1	2	2	1	3	0	-3	4	0
HIPK4	Km app	5	3	9	2	3	-2	7	7	6	9	4
Hyl	Km app	-1	0	-1	2	5	2	-1	-6	1	-2	-4
IGF1R	Km app	8	10	11	-2	-2	-3	0	1	7	8	-2
IKK_alpha	Km app	-16	2	1	-2	0	7	6	-2	0	2	3
IKK_beta	Km app	13	1	5	2	-2	5	-2	7	1	4	1
IKK_epsilon	Km app	4	2	1	2	-6	-2	1	-4	2	0	-2
InsR	Km app	9	6	12	4	4	3	0	6	10	3	-1
IRAK1	Km app	1	-1	51	-3	-3	-8	-5	8	14	3	-5
IRAK4	Km app	14	12	8	6	2	7	10	10	4	10	7
IRR	Km app	14	16	0	7	-12	2	9	-5	2	5	-2
ITK	Km app	81	0	19	13	-5	2	2	22	3	6	-2
JAK1	Km app	-2	-10	23	-8	-9	0	1	14	2	-18	9
JAK2	Km app	1	-4	56	-6	-12	5	-7	13	-3	-9	5
JAK3	Km app	80	5	89	-4	-7	-3	-1	3	-8	-2	2
JNK1_alpha1	NA	9	8	67	5	-2	11	11	16	2	10	3
JNK2	NA	5	5	47	0	2	-1	3	0	-2	3	4
JNK3	NA	5	5	57	6	-1	7	6	14	3	6	4
KDR	Km app	66	60	49	9	8	4	15	8	13	8	3
KHS1	Km app	17	34	3	-9	-15	10	14	19	8	21	18
Kit	Km app	18	21	0	-5	-6	-8	9	23	0	7	-6
Lck	Km app	98	100	23	82	74	33	64	43	26	22	22
LIMK1	NA	41	34	20	14	1	34	9	16	-2	13	2
LRRK2	Km app	-3	1	48	60	-1	-2	-5	0	22	19	9
LTK	Km app	6	7	8	1	-3	-7	2	-2	-5	6	5
Lyn	Km app	97	97	18	38	31	8	33	13	12	23	19
MAP4K4	Km app	12	5	18	9	6	5	20	18	-18	13	20
MAPKAPK2	Km app	8	8	2	-2	-3	9	7	3	2	7	5
MAPKAPK3	Km app	1	-3	-5	-3	-8	6	-7	6	-2	-3	10
MARK1	Km app	9	6	-2	1	1	1	10	5	1	5	11
MARK3	Km app	7	6	2	-3	-5	-6	3	-1	0	7	13
MEK1	NA	40	31	3	15	7	1	2	-3	0	-1	2
MEK3	NA	6	3	9	-2	0	-1	-5	1	2	-3	5
MEKK2	NA	35	37	20	0	-5	1	2	-1	7	-1	4
MELK	Km app	-1	-10	6	-2	0	9	3	10	5	13	7
Mer	Km app	31	42	5	-3	-4	13	6	3	-4	7	2
Met	Km app	12	8	4	5	5	-1	5	1	-2	4	9
Mink1	Km app	21	11	7	27	10	-3	12	9	15	12	23
MKK6	NA	-1	-4	7	5	10	-1	2	10	0	-3	4
MKNK1	Km app	10	1	-3	3	-1	5	2	3	0	6	1
MKNK2	NA	18	24	23	0	3	5	-3	0	-2	5	5
MLK1	Km app	2	0	45	-9	-8	-3	2	8	0	-1	8
MLK2	NA	10	9	37	6	0	-1	4	2	4	-3	1
MRCK_alpha	Km app	3	2	1	-5	0	-3	-4	11	0	13	1
MSK1	Km app	1	-1	9	-2	0	1	3	3	6	4	10
MSSK1	Km app	3	1	-4	5	2	-1	5	2	-3	2	5
MST1	Km app	22	21	14	-1	2	6	4	3	3	-13	-1
MST2	Km app	16	24	2	-7	-7	-3	7	6	-5	12	17
MST3	Km app	14	17	3	9	7	15	6	8	3	-10	4
MST4	Km app	16	21	-12	2	-8	5	8	3	-11	5	2
mTOR	Km app	28	25	7	1	4	4	0	5	-4	-1	5
MuSK	Km app	-12	-1	6	0	-7	10	-9	40	-1	-2	7
MYLK(smMLCK)	NA	-3	-2	4	2	10	-1	-3	1	-5	6	1
MYLK3(caMLCK)	NA	6	10	2	6	2	-1	10	4	1	5	10
NEK1	Km app	-6	-2	6	-13	9	6	6	-5	-2	2	3
NEK4	Km app	4	3	12	0	3	4	1	7	6	1	6
NEK6	Km app	5	11	8	1	-2	19	10	4	7	10	9
NEK9	Km app	2	8	12	-4	-2	-6	1	-10	5	2	0
NLK	NA	5	9	-1	2	1	3	3	1	-2	0	10
p38_alpha(direct)	Km app	6	10	7	-3	0	9	12	4	1	11	3
p38_beta	Km app	8	12	8	1	0	5	9	2	4	8	8
p38_delta	Km app	14	5	10	4	3	6	8	1	10	5	7
p38_gamma	Km app	2	2	5	8	4	5	5	8	6	4	-1
p70S6K	Km app	-1	13	7	-10	5	-6	12	6	0	10	4

		% Inhibition by Inhibitor										
Kinase	**[ATP]**	**1a**	**1b**	**2**	**3a**	**3c**	**4**	**5**	**6**	**7**	**8**	**9**
PAK1	Km app	9	4	-4	-2	0	-2	4	3	4	71	6
PAK3	Km app	19	16	10	3	0	12	2	6	7	0	39
PAK4	Km app	6	6	9	1	-2	-1	16	9	2	2	10
PAK6	Km app	2	1	-9	11	6	3	1	-8	-2	-2	-7
PASK	Km app	1	4	6	-4	-7	2	0	10	2	1	-4
PDGFR_alpha	Km app	50	49	19	0	2	4	0	-4	4	-4	-2
PDK1(direct)	Km app	3	5	7	4	0	10	1	-2	-9	5	8
PhK_gamma1	Km app	3	11	3	-2	1	11	3	5	3	2	-2
PhK_gamma2	Km app	4	0	-1	-3	-4	2	6	3	1	3	-3
PI3K-A	Km app	5	6	3	-12	-15	9	2	32	6	1	1
PI3K-G	Km app	-9	-3	-20	-1	0	3	8	5	-28	5	8
PIM1	Km app	12	13	5	-9	-6	2	13	5	6	23	5
PKA	Km app	4	3	-1	3	1	-1	1	-1	-2	-5	1
PKC_alpha	Km app	7	1	7	0	-2	3	-9	14	-2	3	14
PKC_beta1	Km app	18	11	11	5	4	-9	5	12	4	5	6
PKC_delta	Km app	5	-18	-7	2	-4	9	-2	13	-6	7	11
PKC_epsilon	Km app	4	9	4	4	6	13	7	1	2	2	-16
PKC_eta	Km app	7	5	7	4	6	12	-3	6	6	4	4
PKC_theta	Km app	8	4	9	-5	4	-5	8	13	2	2	17
PKC_zeta	Km app	11	6	3	8	1	15	10	-4	5	10	6
PKD1	Km app	11	9	11	6	0	4	5	6	5	4	1
PKG1_alpha	Km app	4	2	3	-1	-2	1	3	-1	4	2	2
PLK1	Km app	7	4	12	3	1	7	1	5	2	0	-5
PLK2	Km app	3	11	7	-11	-11	0	1	-3	-1	11	8
PLK3	Km app	16	-8	-5	-16	-19	2	3	9	-17	14	7
PRAK	Km app	1	1	-1	4	1	1	-3	-1	-1	2	-2
PRK1	Km app	11	10	8	2	2	1	13	-9	5	8	-2
PRKAA1	Km app	6	1	7	-13	-12	1	-1	5	5	2	8
PrKX	Km app	4	6	4	6	2	3	8	4	8	1	5
RAF1(Y340D,Y341D)	NA	56	47	10	3	5	47	6	0	2	6	5
Ret	Km app	87	84	65	13	11	21	12	15	12	11	4
RIPK2	NA	99	100	3	73	54	60	1	1	0	4	-1
ROCK1	Km app	5	5	1	-5	-9	-2	3	0	-5	-4	-4
ROCK2	Km app	-1	19	-8	-3	-3	4	16	10	-7	6	2
Ron	Km app	4	-6	5	-2	3	4	2	4	-2	3	4
Ros	Km app	-1	-10	48	1	2	9	3	12	2	-15	-2
Rse	Km app	7	6	13	3	1	-1	1	2	3	-4	5
RSK1	Km app	5	5	9	-1	-2	2	4	-2	4	4	-1
RSK2	Km app	-7	-7	6	-4	-1	-2	-13	3	2	-15	16
RSK3	Km app	7	6	15	9	2	3	1	3	1	7	2
SGK1	Km app	4	3	13	-5	-5	1	5	4	1	3	-1
SGK2	Km app	-1	1	-4	3	-2	1	2	3	-3	2	1
SGK3	Km app	-1	-1	0	2	0	5	4	5	-4	3	4
SIK2	Km app	0	6	9	3	1	4	6	5	3	2	-1
SLK	NA	6	12	9	2	0	1	11	6	0	10	1
SPHK1	Km app	9	6	-4	-16	-16	4	5	9	-1	1	22
Src	Km app	98	97	56	49	35	18	83	68	65	57	45
Srm	Km app	105	95	6	29	12	17	12	4	0	6	8
SRPK1	Km app	3	4	0	3	0	-2	0	0	0	2	0
STK16	NA	2	4	96	0	-19	6	-5	7	2	5	2
STK33	NA	14	12	39	-3	3	1	-4	0	4	-3	-2
Syk	Km app	2	-1	35	-1	-3	5	1	2	0	1	6
TAK1-TAB1	NA	2	0	18	0	9	-4	1	-2	4	1	7
TAO1	Km app	-1	-2	8	-1	-1	8	4	1	7	-1	-1
TBK1	Km app	8	4	13	0	0	5	6	2	5	1	8
TEC	NA	100	90	92	91	86	71	37	12	19	20	12
TGFBR1	NA	32	33	27	5	5	3	-1	2	5	7	6
Tie2	Km app	57	45	6	6	1	5	8	10	-6	5	13
TNK2	NA	86	81	26	19	9	5	11	13	4	13	4
TrkA	Km app	24	23	34	16	17	14	17	9	28	22	8
TrkB	Km app	11	9	20	-2	-4	10	7	2	3	3	5
TSSK1	Km app	4	5	6	2	1	3	-3	5	4	6	4
TTK	NA	10	11	49	12	5	-3	6	3	4	7	3
TXK	Km app	93	76	95	89	66	31	3	22	10	11	6
TYK2	Km app	2	1	28	-1	-2	4	7	3	3	5	1
WEE1	NA	1	1	56	5	2	-6	8	4	2	33	8
WNK2	NA	10	9	4	14	1	8	1	1	3	-2	5
Yes	Km app	99	100	20	74	65	22	54	36	39	14	19
YSK1	Km app	6	7	2	-12	5	-3	4	1	-3	-2	-8
ZAK	NA	27	7	2	1	2	4	1	0	4	0	1
ZAP-70	Km app	13	15	-5	5	1	-8	15	-4	2	17	3
ZIPK	Km app	5	5	6	0	-5	5	7	5	2	5	4

Figure S3. a) Close up view of the Btk H3 pocket showing the amino acid residues that line the binding site of inhibitor **9**. b) Sequence alignment of Btk versus kinases that were inhibited by inhibitors **5**–**9** (see Figure S2), and/or kinases that have been reported to form an H3 pocket (ref. *44* of main text). Residue numbers are from the Btk sequence.

a

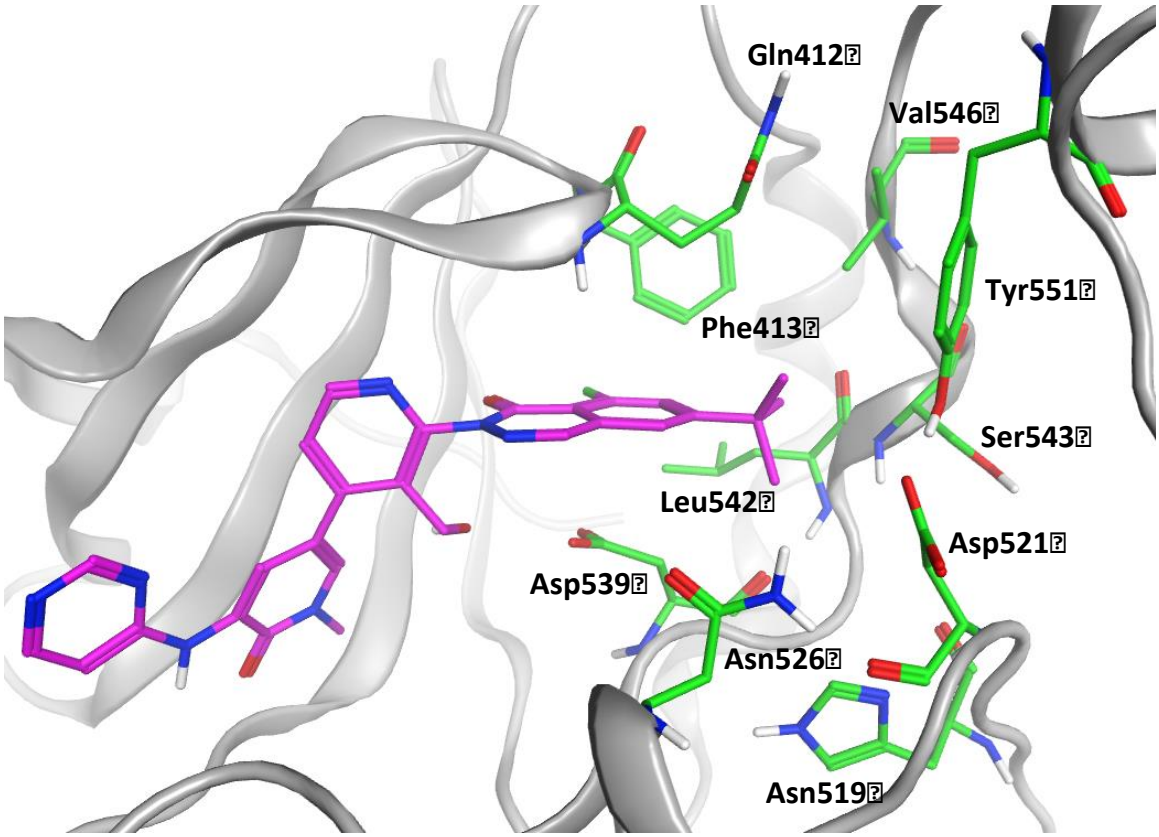

b

	H3 Site Residue Number and Identity									
Kinase	**412**	**413**	**519**	**521**	**526**	**539**	**542**	**543**	**546**	**551**
BTK	Gln	Phe	His	Asp	Asn	Asp	Leu	Ser	Val	Tyr
SRC	Cys	Phe	His	Asp	Asn	Asp	Leu	Ala	Ile	Tyr
FGR	Cys	Phe	His	Asp	Asn	Asp	Leu	Ala	Ile	Tyr
BMX	Gln	Phe	His	Asp	Asn	Asp	Met	Thr	Val	Tyr
ITK	Gln	Phe	His	Asp	Asn	Asp	Met	Thr	Val	Tyr
HCK	Gln	Phe	His	Asp	Asn	Asp	Leu	Ala	Ile	Tyr

REFERENCES

1. Yamamoto, S., and Yoshizawa, T. (2011) Purinone derivative, PCT Int. Appl. WO 2011/152351 A1.

2. Barf, T. A., Jans, C. G. J. M., Man, D. P. A., Oubrie, A. A., Raaijmakers, H. C. A., Rewinkel, J. B. M., Sterrenburg, J.-G., and Wijkmans, J. C. H. M. (2013) 4-Imidazopyridazin-1-yl-benzamides and 4-imidazotriazin-1-yl-benzamides as Btk inhibitors, PCT Int. Appl. WO 2013/010868 A1.

3. Crawford, J. J., Ortwine, D. F., Wei, B., and Young, W. B. (2013) Heteroaryl pyridone and aza-pyridone compounds as inhibitors of Btk activity. PCT Int. Appl. WO 2013/067274.

4. Crawford, J. J., Ortwine, D. F., Wei, B., and Young, W. B. (2013) 8-Fluorophthalazin-1(2H)-one compounds as inhibitors of Btk activity. PCT Int. Appl. WO 2013/067264.

5. Otwinowski, Z., and Minor, W. (1997) Processing of X-ray diffraction data collected in oscillation mode, *Methods Enzymol. 276*, 307–326.

6. Winn, M. D., Ballard, C. C., Cowtan, K. D., Dodson, E. J., Emsley, P., Evans, P. R., Keegan, R. M., Krissinel, E. B., Leslie, A. G., McCoy, A., McNicholas, S. J., Murshudov, G. N., Pannu, N. S., Potterton, E. A., Powell, H. R., Read, R. J., Vagin, A., and Wilson, K. S. (2011) Overview of the CCP4 suite and current developments, *Acta Crystallogr., Sect. D: Biol. Crystallogr. 67*, 235–242.

7. Berman, H. M., Westbrook, J., Feng, Z., Gilliland, G., Bhat, T. N., Weissig, H., Shindyalov, I. N., and Bourne, P. E. (2000) The Protein Data Bank, *Nucleic Acids Res. 28*, 235–242.

8. Emsley, P., Lohkamp, B., Scott, W. G., and Cowtan, K. (2010) Features and development of Coot, *Acta Crystallogr., Sect. D: Biol. Crystallogr. 66*, 486–501.

9. Murshudov, G. N., Skubak, P., Lebedev, A. A., Pannu, N. S., Steiner, R. A., Nicholls, R. A., Winn, M. D., Long, F., and Vagin, A. A. (2011) REFMAC5 for the refinement of macromolecular structures, *Acta Crystallogr., Sect. D: Biol. Crystallogr. 67*, 355–367.

10. Adams, P. D., Afonine, P. V., Bunkoczi, G., Chen, V. B., Davis, I. W., Echols, N., Headd, J. J., Hung, L. W., Kapral, G. J., Grosse-Kunstleve, R. W., McCoy, A. J., Moriarty, N. W., Oeffner, R., Read, R. J., Richardson, D. C., Richardson, J. S., Terwilliger, T. C., and Zwart, P. H. (2010) PHENIX: a comprehensive Python-based

system for macromolecular structure solution, *Acta Crystallogr., Sect. D: Biol. Crystallogr. 66*, 213–221.
11. Paavilainen, V. O., McFarland, J. M., and Taunton, J. (2015) Bruton's tyrosine kinase in complex with a t-butyl cyanoacrylamide inhibitor, PDB 4YHF.